Fullerene-like CdSe nanoparticles

Silvana Botti
Laboratoire des Solides Irradiés,
École Polytechnique, CNRS, CEA-DSM, 91128 Palaiseau, France
LPMCN, Université Claude Bernard Lyon I and CNRS, 69622 Villeurbanne, France
Phone number: + 33 4 72448187
European Theoretical Spectroscopy Facility (ETSF)

silvana.botti@polytechnique.edu

March 10, 2009

Abstract

Cadmium selenide (CdSe) nanocrystals with wurtzite-like core and surface passivated by organic molecules have been extensively studied for the past 20 years and are already used for diverse applications, ranging from light emitting diods, to photovoltaic cells and biological markers. Recently, however, there were experimental and theoretical evidences that pointed to the existence of a novel class of CdSe nanocrystals. These are very small, magic-sized, CdSe nanoparticles with fullerene-like geometry that proved to be extremely stable. This discovery has paved the way to the development of CdSe "cluster-assembled materials" – materials made of three dimensional ordered arrays of size-selected nanoparticles. The enormous potential of these new materials lies in the ability to fine-tune their properties by controlling the size of the constituent nanoparticles, combined with the novel collective behavior arising from the creation of nanoparticle arrays.

keywords: CdSe nanoparticles, fullerenes, *ab initio* calculations

Contents

1 Introduction

Cadmium selenide (CdSe) is a binary compound made of cadmium and selenium, that crystallizes in the hexagonal closed-packed wurtzite structure. Its optical band gap measures 1.85 eV at low temperature (Dai et al. 2007b). Current research on CdSe has focused mostly on nanoparticles, i.e., small portions cut out from bulk CdSe, with diameters between 1 and 100 nm. The interest in these nanosized systems can be understood by their special properties, significantly different from the properties of the parent bulk compound, that open the possibility of novel technological applications. Furthermore, the very small size of these nanoparticles makes them particularly suited for miniaturization purposes. In fact, while the miniaturization of conventional silicon-based electronics is approaching fundamental performance limits, researchers are actively working to find new nanosized materials that are able to overcome these limits.

All nanoparticles exhibit a fundamental property known as "quantum confinement" (Bawendi et al. 1990), due to the modification of the energy states of electrons confined in a very small volume. Quantum confinement is dependent on the confinement volume, i.e., on the size of the nanoparticle. This means that the electronic properties of CdSe nanoparticles can be tailored by controlling their size. As a consequence, CdSe nanoparticles have size-tunable absorption and luminescence spectra. This characteristic makes them particularly attractive to be employed in optical devices, such as in light-emitting diodes that have to cover a large part of the visible spectrum (Coe et al. 2002, Bowers et al. 2005). Along the same lines, CdSe nanoparticles have already proved to be excellent components for a variety of applications, such as in optically pumped lasers (Tessler et al. 2002), photovoltaic cells (Klimov 2003, Greenham et al. 1996), telecommunications (Harrison et al. 2000), and in biomedicine as chemical markers (Bruchez et al. 1998, Michalet et al. 2005).

The common requirement that makes possible all these different applications of CdSe nanoparticles is the high proficiency achieved in the control of a remarkably narrow size distribution (even lower than 5% (Murray et al. 1993)) during the synthesis process. In fact, it is the size distribution that determines the sharpness of the optical peaks. A further advantage of CdSe nanocrystals is the degree of efficiency attained in their synthesis, the high quality of the resulting samples, and the fact that the optical gap is in the visible range. In most common experimental setups, CdSe nanoparticles are formed by kinetically controlled precipitation, and are terminated with capping organic ligands, like, e.g., the trioctyl phosphine oxide (TOPO) molecule, which provide stabilization of the otherwise reactive dangling orbitals at the surface (Murray et al. 1993). High quality colloidal CdSe nanoparticles have been routinely synthesized for more than a decade: their sizes range from 1 nm to hundreds of nm and their core displays the same symmetry as wurtzite.

The electronic states of any nano-object are also sensitive to the overall cluster shape, and more specifically to the deformations due to surface reconstruction, to the presence of defects, and to the symmetry properties of the arrangement of atoms in the core (Peng et al. 2000). These geometrical details are of course more critical when the cluster is very small, i.e., when the surface/volume ratio is the largest. In particular, defects and dangling bonds are essentially localized at the surface. Moreover, for practical uses, further requirements, such as a high chemical stability of the nanostructure and an enhanced photoluminescence intensity, are of utmost importance. Unfortunately, these characteristics are inhibited by the presence of defects. As a consequence, often the quantum yields for very small CdSe nanoparticles in solution turn out to be below 1% (Bruchez et al. 1998, Chan and Nie 1998). The reason is that these colloidal nanoparticles contain a large number of defects, especially at the surface, where radiationless recombination of the charge carriers can occur. Therefore, controlling the quality of the growth of small clusters, and in particular controlling the formation of dangling bonds

at their surface, is essential for any kind of application.

In this context, the recent synthesis and probable identification of the very small, and highly stable, $(CdSe)_{33}$ and $(CdSe)_{34}$ nanoparticles grown in a solution of toluene (Kasuya et al. 2004, 2005) came as a breakthrough. The experimental absorption spectra of these nanoparticles at low temperature exhibit sharp peaks, similar to the ones that characterize TOPO-capped clusters of the same size (Murray et al. 1993). However, the surfactant molecules employed in the synthesis process are, in this case, removed by laser vaporization. Furthermore, an X-ray analysis indicates that the coordination number of Se is between 3 (the coordination of a fullerene) and 4 (the coordination of the bulk crystal). In view of this, and in absence of direct structural data, the non-passivated compound nanoparticles were predicted to have a core-cage structure, composed by a puckered fullerene-like $(CdSe)_{28}$ cage accommodating a $(CdSe)_n$ (n=5,6) wurtzite unit inside (see Fig. 1). Further ab initio calculations of structural and optical properties validated this interpretation (Kasuya et al. 2004, Botti and Marques 2007).

These very small fullerene-like systems, in the size range of 1–2 nm, are particularly interesting, as they have an increased probability to take the form of magic-sized nanocrystals, leading to ultra-stable single sized ensembles, which are in principle characterized by very sharp absorption peaks. The concept of magic-size has been well known for several years in the field of metal clusters, but it is less common for semiconductor nanoparticles.

Furthermore, the recent discovery of CdSe and other fullerene-like semiconducting cluster has renewed the interest for the so-called "cluster-assembled materials". In fact, cluster-assembled materials form one of the most promising frontiers in the design of nano-devices. They are composed by three dimensional arrays of ultrastable size-selected nanoparticles, organized in a similar way as atoms are organized to form a crystal. Cluster-assembled materials ideally combine the properties of the single nano-object with novel collective behaviors arising from the periodic arrangement of the solid. Of course, the interaction between clusters cannot be too strong, such to destroy the discrete nature of the optical transitions. This means that the surface of the cluster has to be well saturated, with no dangling bonds. Unfortunately, up to now most attempts to design cluster-assembled matter have lead to metastable materials, which can be stabilized only by a dielectric matrix that prevents the individual clusters from reacting with their neighbors. Only few cluster materials are known at present, the most famous are made of carbon fullerenes (C_{60} and C_{70}). However, the recently synthesized CdSe fullerenes are very small clusters (1.5 nm of diameter), extremely stable, and which can be produced in macroscopic quantities: all these characteristics point to the possibility of using them to produce new cluster-assembled materials.

2 Synthesis and spectroscopic characterization

Numerous approaches (Katari et al. 1994, Hines and Guyot-Sionnest 1996, Chen et al. 1997, Peng et al. 1997, Dabbousi et al. 1997, Peng et al. 2000, Mikulec and Bawendi 2000, Peng and Peng 2001, Talapin et al. 2001, Gaponik et al. 2002a,b, Reiss et al. 2002, Yu et al. 2003b, Zhang et al. 2003, Yu et al. 2003b,a, Zhong et al. 2004, Dai et al. 2006, Pradhan et al. 2006) have been developed to synthesize highly crystalline and monodisperse II-VI semiconductor nanocrystals, following the path opened by Murray et al. (Murray et al. 1993). However, these approaches are mostly suitable to produce regular-sized nanocrystals (>2 nm), but cannot be commonly employed to synthesize magic-size small clusters (1–2 nm). In particular, in the magic size regime, a large percentage of the atoms are at the surface, which makes the control of dangling bonds much more important.

Very small CdSe nanocrystals have been synthesized by the over-layering method (Soloviev et al. 2000), the etching preparation starting from larger nanocrystals (Landes et al. 2001), and

the reverse-micelle approach (Kasuya et al. 2004). Peculiar optical properties were obtained by magic-size nanoparticles grown by hot injection (Bowers et al. 2005): these ultra-small clusters exhibit broadband emission (420–710 nm) throughout most of the visible light spectrum, while not suffering from self-absorption. This property makes them ideal materials to produce white-light LED's. In general, it is assumed that these clusters are saturated with ligands, even if there is direct information about the reconstruction at the surface.

However, ligand-free fullerene-like core-cage particles were for the first time produced by Kasuya et al. (Kasuya et al. 2004, 2005) only in 2004. Since then, other groups tested new reproducible and controllable methods to grow in solution magic-sized small CdSe clusters. The exact control of the size of the nanocrystal and the sharpness of the optical peaks are both essential for any practical application. Of course, also the stability in time of the clusters is an important parameter to consider.

Kudera et al. (Kudera et al. 2007) reported a method for controlling the sequential growth of CdSe clusters in solution that yields only magic-size nanocrystals of progressively larger sizes. The resulting nano-objects are characterized by sharp optical absorption spectra with peaks at well defined energies, in agreement with the ones reported by Kasuya et al. (Kasuya et al. 2004). Also the cluster sizes, estimated by X-ray diffraction analysis, are compatible with the findings of Kasuya et al. (Kasuya et al. 2004). Further transmission electron microscopy analysis revealed that all clusters are roughly spherical and that they are not aggregated. The mechanism of growth is determined by the competition between the attachment and detachment of single atoms at the surface. Once a cluster has grown to a magic size, its structure is so stable that no atom can detach from it. Therefore, it can only grow further, but it cannot shrink. This growth mechanism is compatible with the creation of cage-like structures, even if there is no direct proof of the fact that fullerene-like clusters are actually produced in this experiment. Unfortunately, these clusters have rather weak luminescence properties. Kudera et al. (Kudera et al. 2007) also proved that the optical properties of their clusters could be improved by passivating their surfaces with a ZnS shell.

Dai et al. (Dai et al. 2007a) reported an injection approach for the synthesis of nanocrystals with long existence period, using cheap cadmium oleate as the source of cadmium. The resulting CdSe clusters are saturated by ligands. They exhibit strong and fixed absorption features and a narrow red-shifted emission. Higher injections/growth temperatures favor a white light emission, but also transform the magic-size nanocrystals into regular-size ones. This same approach was also used by them to synthesize CdTe clusters.

On the other hand, Ouyang et al. (Ouyang et al. 2008) used a non-injection one-pot synthetic approach to achieve colloidal CdSe ensembles consisting of single-sized nanocrystals exhibiting bright bandgap photoluminescence emission. Their systematic study suggests that the growth of large CdSe clusters is favored by long ligands at high growth temperature, while the growth of small CdSe magic-size clusters is favored by short ligands at low growth temperature.

Finally, Kuçar et al. (Kucur et al. 2008) reported an efficient top-down synthesis in an amine-rich solution of small stable CdSe nanocrystals. They are produced by decomposition of initial nanocrystals within several days. The most stable clusters were characterized by spectroscopic methods and the comparison of absorption and photoluminescence spectra with previous studies suggests a predominant cage-like structure. The analysis of the absorption peaks revealed a preferred synthesis of $(CdSe)_{33,34}$ clusters. The emission decay rate of these clusters is comparable with that of organic dyes.

Despite the important contributions coming from all these recent studies, the preparation and understanding of highly luminescent, thermodynamically stable, small size CdSe clusters is still at the beginning. We are optimistic, however, that the next few years will bring new optimized techniques for the production of these clusters, that will open the way for development

of the exciting and innovative applications that have already been foreseen.

3 Ab initio calculations

From the theoretical side, it is desirable to obtain from reliable calculations all possible complementary information on the atomic arrangement and surface deformation of CdSe clusters, in order to understand and complement experimental evidences. In fact, experimental measurements alone are usually not able to provide conclusive results concerning the surface reconstruction and the role of passivating ligands. Moreover, theoretical calculations can give a deeper insight on how surface reconstructions produce modifications of the electronic states, and consequently of the optical properties at the basis of all technological applications.

For ligand-terminated small and regular-size CdSe clusters, transmission electron microscopy data (Murray et al. 1993, Shiang et al. 1995), molecular dynamics simulations or first-principles techniques without self-consistency (Rabani 2001, Sarkar and Springborg 2003), and self-consistent *ab initio* structural relaxations (Puzder et al. 2004, Botti and Marques 2007) agree on predicting an atomic arrangement of the inner Cd and Se atoms analogous to the one in the wurtzite CdSe crystal. The extent to which the cluster surface retains the crystal geometry is more controversial as the surface cannot be easily resolved experimentally. Generally, if the surface is properly passivated, the reconstruction is assumed to be small and limited to the outermost layer (and eventually the layer just beneath it), which is in agreement with molecular dynamics simulations (Rabani 2001). However, Puzder *et al.* (Puzder et al. 2004) recently predicted for clusters with diameters up to 1.5 nm a strong surface reconstruction, remarkably similar in vacuum and in the presence of passivating ligands.

The core-cage structures proposed by Kasuya et al. (Kasuya et al. 2004) are significantly different from all bulk-derived arrangements previously studied. These geometries were found to be particularly stable by first-principles total energy calculations (Kasuya et al. 2004, Botti and Marques 2007). Furthermore, calculations of optical spectra (Botti and Marques 2007) have offered a definitive proof for the identification of the observed nanoparticles with the fullerene-like structures, through the comparison between measured (Kasuya et al. 2004) and simulated spectra. In fact, as the electronic states (and, as a consequence, absorption or emission peaks) are strongly modified by changes of size and shape, optical spectroscopy can thus be a powerful tool (especially if it can be combined with other spectroscopic techniques) to probe the atomic arrangement of synthesized nanoparticles.

In the following of this section we will discuss how the well-known density functional theory (DFT) (Hohenberg and Kohn 1964) has been applied to access information concerning the structural and electronic properties of CdSe fullerenes. Moreover, we will see how the comparison between theoretical and experimental results provides a deeper insight into the properties of complex nanostructured materials.

We chose to restrict our discussion to DFT, as it is the most popular and versatile method available in condensed-matter physics, computational physics, and computational chemistry. Compared to empirical or semi-empirical approaches, DFT has a total absence of parameters fitted to experimental data. This characteristic is essential to guarantee predictive power to any theory. Furthermore, within first principles (i.e. parameter free) approaches, DFT is relatively light from a computational perspective. In fact, in contrast with traditional methods in electronic structure theory, in particular Hartree-Fock theory and its descendants, DFT is not aiming at finding a good approximation for the complicated many-electron wavefunction: the electronic density becomes the key quantity at the heart of the theory. Whereas the many-body wavefunction is dependent on $3N$ variables (without considering spin), three spatial variables for each of the N electrons, the density is only a function of three variables and is a simpler

quantity to deal with, both conceptually and practically. For practical purposes, DFT is usually implemented in the Kohn-Sham scheme (Kohn and Sham 1965), which makes use of a non-interacting system yielding the same density as the original problem. For a review on the basics of DFT we suggest the reader to look at the rich literature on the subject (Dreizler and Gross 1995, Parr and Yang 1989, Fiolhais et al. 2003).

3.1 Structures of energetically stable CdSe nanoparticles

The atomic positions of CdSe nanoparticles can be routinely obtained by geometry optimization using any quantum chemistry or solid state physics code. The starting point of any structural optimization procedure is to consider a series of candidate structures with different geometries and sizes. Here we consider $(CdSe)_n$ aggregates with sizes ranging up to about 1.5 nm. To build these atomic arrangements it is possible to start from three different kinds of ideal geometries: (i) bulk fragments cut into the infinite wurtzite crystal, (ii) octahedral fullerene-like cages made of four and six-membered rings and (iii) the core-cage structures of Ref. (Kasuya et al. 2004), composed of puckered CdSe fullerene-type cages which include $(CdSe)_n$ wurtzite units of adequate size to form a three-dimensional network. Following Ref. (Botti and Marques 2007), we can assume that the Cd-Se distance before structural relaxation is the distance in the CdSe wurtzite crystal, calculated within DFT (Soler et al. 2002) in the same approximations used for the nanoparticles: its value (0.257 nm) compares well with the experimental value (0.263 nm).

In the following we will analyze as an illustration the structural calculations of Ref. (Botti and Marques 2007), comparing them with the analogous DFT calculations for wurtzite-like clusters of Ref. (Puzder et al. 2004) and for core-cage clusters of Ref. (Kasuya et al. 2004). Botti and Marques (Botti and Marques 2007) used an implementation of DFT (Soler et al. 2002) within the local density approximation (LDA) (Perdew and Zunger 1981) for the exchange and correlation potential and norm-conserving pseudopotentials (Hamann 1989, Troullier and Martins 1991). Puzder et al. (Puzder et al. 2004) used a similar technique, but with another implementation of DFT (Gygi, F. 1999). Finally, Kasuya et al. (Kasuya et al. 2004) performed DFT calculations (Kresse and Furthmuller 1996) using ultrasoft pseudopotentials (Vanderbilt 1990) and the generalized gradient approximation (GGA) (Perdew et al. 1996) for the exchange-correlation potential.

Atomic arrangements after optimization using DFT are depicted in Fig. 2 (see (Botti and Marques 2007)). All clusters suffer contraction upon geometry minimization. For example, $(CdSe)_{33,34}$ clusters experience a size reduction of about 1–1.5%. The theoretical results are in agreement with the X-ray analysis of (Kasuya et al. 2004). However, as the relaxation affects mainly the outermost atoms, the overall effect is more pronounced in smaller structures, where the average Cd-Se distance decreases up to 4%. This contraction does not conserve the overall shape, as Cd atoms are pulled inside the cluster and Se atoms are puckered out. As a consequence, Cd-Cd average distances can be reduced by 30%, while Se-Se distances remain essentially unvaried. This is clearly visible in Fig. 3, where the relaxed distance of Cd (circles) and Se (diamonds) atoms from the center of the cluster is plotted for $(CdSe)_{33,34}$ clusters as a function of their distance before relaxation. If the atoms remained in their initial position, all data points would fall on the straight line $y = x$. The fact that most Cd atoms lie below the line, while most Se atoms are above it, shows that in our simulation Cd atoms prefer to move inward and Se atoms outward. That puckering happens independently of the cluster size (Kasuya et al. 2004, Puzder et al. 2004, Botti and Marques 2007).

All wurtzite fragments get significantly distorted upon relaxation and break their original symmetry. However, the strong modification of bond lengths and angles concerns essentially the surface layer (Puzder et al. 2004, Botti and Marques 2007). In particular, we can see

in Fig. 3(a) that the wurtzite-type $(CdSe)_{33}$ is already large enough to conserve a bulk-like crystalline core. In fact, the spread of the points from the straight line is pronounced only for the external shell of atoms. The calculated overall contraction of the cluster is consistent with experimental data (Zhang et al. 2002). Also the empty cages [$(CdSe)_{12}$, $(CdSe)_{28}$, and $(CdSe)_{48}$] get puckered, but conserve their overall shape. Their binding energies are smaller by about 0.1 eV per CdSe unit with respect to the binding energies of the corresponding filled cages [see Fig. 4(a)], showing the importance of preserving the three-dimensional sp^3 Cd-Se network.

Models based only on the wurtzite structure of bulk CdSe fail to predict the existence of stable "magic clusters" with well defined sizes and number of atoms. In contrast, the core-cage structures proposed by Kasuya et al. can appear only for well defined sizes and number of atoms, as fullerene cages can be built only for 12, 16, 28, 48, 76, etc. atoms and only some of these cages can be filled conveniently with wurtzite-coordinated CdSe units. To optimize the core-cage structures [$(CdSe)_{12+1=13}$,$(CdSe)_{28+5=33}$, and$(CdSe)_{28+6=34}$] Botti and Marques (Botti and Marques 2007) created different starting arrangements assuming different orientations for the encapsulated $CdSe_{n=1,5,6}$ units. In the relaxed assemblies the distributions of bond lengths and angles result very similar despite of the distinct initial configurations. The fact that the surfaces of core-cage clusters do not show neither strong reconstruction nor deleterious dangling bonds, in contrast with surfaces of wurtzite-like cluster not cured by passivation, explains why fullerene-like CdSe clusters are particularly non-reactive and prevent them from merging together to form larger clusters. This is crucial to have promising building blocks for three-dimensional cluster solids.

The right panel of Fig. 4 shows the DFT Kohn-Sham gap between the highest occupied and lowest unoccupied molecular orbitals (HOMO-LUMO) for a series of clusters of different types: wurtzite, cages, and filled cages. Both empty and filled cages exhibit much larger HOMO-LUMO gaps than their wurtzite counterparts, indicating therefore that there are no dangling bonds at their surface. In the left panel we show the results from (Kasuya et al. 2004) for the binding energy of the filled cages. The two most stable structures are clearly $(CdSe)_{33}$ and $(CdSe)_{34}$. It is curious that the first is significantly more deformed under optimization than $(CdSe)_{34}$, but it turns out to have a very similar binding energy. The filled cage structure made of 13 units gives as well a relative minimum in the total energy per pair (Botti and Marques 2007). In the case of $(CdSe)_{13}$ and $(CdSe)_{33}$ it is possible to compare the total energies of the different three-dimensional isomers (Botti and Marques 2007): the core-cage nanoparticles have a slightly higher binding energy per CdSe unit [0.15 eV for $(CdSe)_{13}$ and 0.05 eV for $(CdSe)_{33}$]. However, we should not forget that the energy differences we are discussing here are all very tiny, sometimes of the same order of magnitude as the accuracy of the calculations. That fact confirms how difficult it can be to extract structural information from a single number (the total energy) and leads to the conclusion that the simple analysis of total energy differences cannot be considered conclusive to demonstrate the existence of fullerene-like CdSe clusters.

3.2 Optical absorption spectra

From the relaxed geometries it is possible to obtain the optical spectra at zero temperature using time-dependent density functional theory (TDDFT) (Runge and Gross 1984, Gross and Kohn 1985). TDDFT is an exact reformulation of time-dependent quantum mechanics, where the fundamental variable is no longer the many-body wave-function but the time-dependent density. It can be viewed as an extension of DFT to the time-dependent domain to describe what happens when a time dependent perturbation is applied. For a review on the subject of time-dependent density functional theory, we suggest the reader to have a look at the rich literature on the subject (Marques et al. 2006, Marques and Gross 2004, Botti et al. 2007).

For the calculation of the photoabsorption cross section Botti and Marques (Botti and Marques 2007) employed a real-time TDDFT approach (Marques et al. 2003, Castro et al. 2006), based on the explicit propagation of the time-dependent Kohn-Sham equations. In this approach, one first excites the system from its ground state by applying a delta electric field $E_0\delta(t)\mathbf{e}_m$. The unit vector $\mathbf{e}_m$ determines the polarization direction of the field, and E_0 its magnitude, which must be small if one is interested in linear response. The reaction of the non-interacting Kohn-Sham system to this sudden perturbation can be readily computed: each ground state Kohn-Sham orbital $\varphi_i^{\mathrm{GS}}(\mathbf{r})$ is instantaneously phase-shifted: $\varphi_i(\mathbf{r}, t = 0^+) = e^{\mathrm{i}E_0\mathbf{e}_m\cdot\mathbf{r}}\varphi_i^{\mathrm{GS}}(\mathbf{r})$. The Kohn-Sham equations are then propagated forward in real time, and the time-dependent density $n(\mathbf{r}, t)$ can then be readily computed. The induced dipole moment variation is an explicit functional of the density:

$$\delta\mathbf{D}^m(t) = \delta\langle\hat{\mathbf{R}}\rangle(t) = \int \mathrm{d}^3r \ [n(\mathbf{r}, t) - n(\mathbf{r}, t = 0)]\,\mathbf{r}\,. \tag{1}$$

The superindex m reminds that the perturbation has been applied along the m-th cartesian direction. The components of the dynamical dipole polarizability tensor $\underline{\alpha}(\omega)$ are directly related to the Fourier transform of the induced dipole moment function:

$$\alpha_{mn}(\omega) = \frac{\delta D_n^m(\omega)}{E_0}\,. \tag{2}$$

The spatially averaged absorption cross section is trivially obtained from the imaginary part of the dynamical polarizability:

$$\sigma(\omega) = \frac{4\pi\omega}{c}\Im\left[\alpha(\omega)\right]\,, \tag{3}$$

where α is the spatial average, or trace, of the tensor

$$\alpha(\omega) = \frac{1}{3}\mathrm{Tr}\left[\underline{\alpha}(\omega)\right]\,. \tag{4}$$

Here we will discuss the results for the excitation energies and the optical spectra of Botti and Marques (Botti and Marques 2007), obtained using TDDFT within the adiabatic local density approximation (ALDA) (Gross and Kohn 1985). These are the only calculations on CdSe clusters available in literature that go beyond the simple application of Fermi's golden rule, i.e. the sum of independent single particle transitions from occupied to empty states (in this case, Kohn-Sham one-particle states). It is well known that the simpler approach of taking the differences of eigenvalues between Kohn-Sham orbitals gives peaks at lower frequencies in disagreement with the experimental spectra (Castro et al. 2002). On the other hand, TDDFT within the ALDA typically reproduces the low energy peaks of the optical spectra with an average accuracy usually below 0.2 eV. The accuracy in reproducing transitions of intermediate energy is known to be somewhat deteriorated, due to the wrong asymptotic behavior of the LDA exchange-correlation potential. For this reason, we focus the analysis of the spectra on the lowest energy peaks.

In Fig. 5 we display the photoabsorption spectra of the empty cages of different diameters, as calculated by Botti and Marques (Botti and Marques 2007). It is clear from the figure that the absorption threshold is systematically blue-shifted with respect to the bulk optical gap ($\simeq$ 1.8 eV). This blue-shift is due to the well-known quantum confinement effects, so it is not surprising that the shift increases with decreasing cluster size. Second, we can compare the absorption threshold with the Kohn-Sham HOMO-LUMO gap shown in the right panel of Fig. 4: the Kohn-Sham gap is systematically smaller than the TDDFT absorption threshold. This is a common observation as the Kohn-Sham transition energies are usually at lower frequencies than

the experimental peaks. We note that the TDDFT optical gaps include both electron-electron and electron-hole corrections to the Kohn-Sham gap at the level of the adiabatic local density approximation.

We should keep in mind that the opening of the gap due to confinement can be counterbalanced by a closing of the gap due to surface reconstruction. This leads to a non trivial dependence of the absorption gap as a function of the cluster size. This effect is already present at the Kohn-Sham level [see the right panel of Fig. 4(a)] and it persists in TDDFT spectra. In fact, the calculated absorption curves are strongly dependent not only on the cluster size but also on the details of its atomic arrangement. This is evident if we compare the optical response of the different isomers of $(CdSe)_{13}$ in Fig. 6 and of $(CdSe)_{33}$ in Fig. 7 (Botti and Marques 2007).

The absorption threshold is lower in wurtzite-type clusters since the HOMO-LUMO gap is reduced due to the presence of defect states in the gap as a consequence of the strong surface deformation. For a similar reason, the larger surface deformation of the core-cage $(CdSe)_{33}$ aggregate in comparison with the more stable $(CdSe)_{34}$ structure explains why the first starts absorbing at lower energies than the second. Finally, we note that the similar curves of different colors in Fig. 7 correspond to distinct core-cage geometries obtained in various optimization simulations. We conclude that the dependence of the relevant peak positions and shapes on the different atomic arrangements is not negligible, but the peak positions and oscillator strengths are sufficiently defined for the purpose to distinguish different geometries by comparing photoabsorption spectra.

A comparison between calculated (Botti and Marques 2007) and measured spectra (Kasuya et al. 2004) is possible for nanoparticles made of 33 and 34 CdSe units (see Fig. 7). The magenta dots refer to room temperature absorption data for mass-selected nanoparticles prepared in toluene at 45°C (sample I), while the orange crosses correspond to analogous data for the solution prepared at 80°C (sample II). Both samples are characterized by strong absorption at 3 eV. For sample II the experimental data show the appearance of a broad peak extending to lower energies. This peak turns out to move to even lower energies when the temperature and the time in the synthesis process increase. In a simple quantum confinement picture, these findings suggest that larger particles, possibly reconstructed bulk fragments, are formed when the temperature increases. Moreover, the sharp peak at about 3 eV, which is always present, was hypothesized to be the signature of the highly resistant fullerene-like clusters.

The calculated spectra (Botti and Marques 2007) shown in Fig. 7 prove the presence of fullerene-like core-cage structures. The theoretical optical response of all model core-cage $(CdSe)_{34}$ clusters is indeed characterized by a well defined absorption peak at 3 eV. Also the core-cage $(CdSe)_{33}$ cluster and the $(CdSe)_{33}$ reconstructed bulk fragment can contribute to this peak. However, they cannot be present in sample I, as that would be signaled by the appearance of a broader peak at lower energy, which is absent in the experimental spectrum. On the other hand, a peak at about 2.5 eV, connected to the peak at 3 eV by a region of increasing absorption, is present in the spectrum for sample II. Our calculations show that the $(CdSe)_{33}$ wurtzite fragment is responsible for the peak at 2.5 eV, while the broad absorption region between 2.5 eV and 3 eV can be explained by the presence of $(CdSe)_{33}$ core-cage structures. This is in disagreement with the intuition of Ref. (Kasuya et al. 2004) that bulk fragments of about 2.0 nm gave rise to the broad absorption below 3 eV.

In summary, by comparing our theoretical spectra with measurements, Botti and Marques (Botti and Marques 2007) could confirm the existence of the stable core-cage fullerene-like structures hypothesized in the seminal work of Kasuya et al. (Kasuya et al. 2004).

4 Conclusions

The use of CdSe fullerene-like nanoparticles for technological applications in the field of cluster-assembled materials is a promising challenge for materials science. To this purpose, there is much work in progress to optimize the production procedures of magic-size small CdSe clusters. Concerning the characterization and the understanding of electronic excitations in these novel nanostructured materials, the combination of experimental and theoretical spectroscopic techniques has proved to be essential to extract reliable and conclusive information on their structural and optical properties.

References

Bawendi, M., Steigerwald, M. and Brus, L., 1990. The quantum-mechanics of larger semiconductor clusters (quantum dots), *Annual Review of Physical Chemistry* 41: 477–496.

Botti, S. and Marques, M. A. L., 2007. Identification of fullerene-like CdSe nanoparticles from optical spectroscopy calculations, *Physical Review B* 75.

Botti, S., Schindlmayr, A., Del Sole, R. and Reining, L., 2007. Time-dependent density-functional theory for extended systems, *Reports on Progress in Physics* 70: 357–407.

Bowers, M., McBride, J. and Rosenthal, S., 2005. White-light emission from magic-sized cadmium selenide nanocrystals, *Journal of the American Chemical Society* 127: 15378–15379.

Bruchez, M., Moronne, M., Gin, P., Weiss, S. and Alivisatos, A., 1998. Semiconductor nanocrystals as fluorescent biological labels, *Science* 281: 2013–2016.

Castro, A., Appel, H., Oliveira, M. et al., 2006. octopus: a tool for the application of time-dependent density functional theory, *Physica Status Solidi B - Basic Solid State Physics* 243: 2465–2488.

Castro, A., Marques, M., Alonso, J., Bertsch, G., Yabana, K. and Rubio, A., 2002. Can optical spectroscopy directly elucidate the ground state of C-20?, *Journal of Chemical Physics* 116: 1930–1933.

Chan, W. and Nie, S., 1998. Quantum dot bioconjugates for ultrasensitive nonisotopic detection, *Science* 281: 2016–2018.

Chen, W., Wang, Z., Lin, Z. and Lin, L., 1997. Absorption and luminescence of the surface states in ZnS nanoparticles, *Journal of Applied Physics* 82: 3111–3115.

Coe, S., Woo, W., Bawendi, M. and Bulovic, V., 2002. Electroluminescence from single monolayers of nanocrystals in molecular organic devices, *Nature* 420: 800–803.

Dabbousi, B., RodriguezViejo, J., Mikulec, F. et al., 1997. (CdSe)ZnS core-shell quantum dots: Synthesis and characterization of a size series of highly luminescent nanocrystallites, *Journal of Physical Chemistry B* 101: 9463–9475.

Dai, Q., Li, D., Chang, J. et al., 2007a. Facile synthesis of magic-sized CdSe and CdTe nanocrystals with tunable existence periods, *Nanotechnology* 18.

Dai, Q., Li, D., Chen, H. et al., 2006. Colloidal CdSe nanocrystals synthesized in noncoordinating solvents with the addition of a secondary ligand: Exceptional growth kinetics, *Journal of Physical Chemistry B* 110: 16508–16513.

Dai, Q., Song, Y., Li, D. et al., 2007b. Temperature dependence of band gap in CdSe nanocrystals, *Chemical Physics Letters* 439: 65–68.

Dreizler, R. and Gross, E. K. U., 1995. *Density functional theory*. New York: Plenum Press.

Fiolhais, C., Marques, M. A. L. and Nogueira, F., ed., 2003. *A primer in density functional theory*, volume 602 of *Lecture Notes in Physics*. Berlin: Springer.

Gaponik, N., Talapin, D., Rogach, A., Eychmuller, A. and Weller, H., 2002a. Efficient phase transfer of luminescent thiol-capped nanocrystals: From water to nonpolar organic solvents, *Nano Letters* 2: 803–806.

Gaponik, N., Talapin, D., Rogach, A. et al., 2002b. Thiol-capping of CdTe nanocrystals: An alternative to organometallic synthetic routes, *Journal of Physical Chemistry B* 106: 7177–7185.

Greenham, N., Peng, X. and Alivisatos, A., 1996. Charge separation and transport in conjugated-polymer/semiconductor-nanocrystal composites studied by photoluminescence quenching and photoconductivity, *Physical Review B* 54: 17628–17637.

Gross, E. and Kohn, W., 1985. Local density-funcional theory of frequency-dependent linear response, *Physical Review Letters* 55: 2850–2852.

Gygi, F., 1999. GP code version 1.16.0 (F. Gygy, LLNL 1999-2004).

Hamann, D., 1989. Generalized norm-conserving pseudopotentials, *Physical Review B* 40: 2980–2987.

Harrison, M., Kershaw, S., Burt, M. et al., 2000. Colloidal nanocrystals for telecommunications. Complete coverage of the low-loss fiber windows by mercury telluride quantum dots, *Pure and Applied Chemistry* 72: 295–307, 1st IUPAC Workshop on Advanced Material (WAM1), HONG KONG, PEOPLES R CHINA, JUL 14-18, 1999.

Hines, M. and Guyot-Sionnest, P., 1996. Synthesis and characterization of strongly luminescing ZnS-Capped CdSe nanocrystals, *Journal of Physical Chemistry* 100: 468–471.

Hohenberg, P. and Kohn, W., 1964. Inhomogeneous electron gas, *Physical Review B* 136: B864–&.

Kasuya, A., Noda, Y., Dmitruk, I. et al., 2005. Stoichiometric and ultra-stable nanoparticles of II-VI compound semiconductors, *European Physical Journal D* 34: 39–41, 12th International Symposium on Small Particles and Inorganic Clusters, Nanjing, PEOPLES R CHINA, SEP 06-10, 2004.

Kasuya, A., Sivamohan, R., Barnakov, Y. et al., 2004. Ultra-stable nanoparticles of CdSe revealed from mass spectrometry, *Nature Materials* 3: 99–102.

Katari, J., Colvin, V. and Alivisatos, A., 1994. X-ray photoelectron-spectroscopy of CdSe nanocrystals with applications to studies of the nanoscrystal surface, *Journal of Physical Chemistry* 98: 4109–4117.

Klimov, V., 2003. Nanocrystal quantum dots, *Los Alamos Sci.* 28: 214.

Kohn, W. and Sham, L., 1965. Self-consistent equations including exchange and correlation effects, *Physical Review* 140: 1133–&.

Kresse, G. and Furthmuller, J., 1996. Efficient iterative schemes for ab initio total-energy calculations using a plane-wave basis set, *Physical Review B* 54: 11169–11186.

Kucur, E., Ziegler, J. and Nann, T., 2008. Synthesis and spectroscopic characterization of fluorescent blue-emitting ultrastable CdSe clusters, *Small* 4: 883–887.

Kudera, S., Zanella, M., Giannini, C. et al., 2007. Sequential growth of magic-size CdSe nanocrystals, *Advanced Materials* 19: 548.

Landes, C., Braun, M., Burda, C. and El-Sayed, M., 2001. Observation of large changes in the band gap absorption energy of small CdSe nanoparticles induced by the adsorption of a strong hole acceptor, *Nano Letters* 1: 667–670.

Marques, M., Castro, A., Bertsch, G. and Rubio, A., 2003. Octopus: a first-principles tool for excited electron-ion dynamics, *Computer Physics Communications* 151: 60–78.

Marques, M. and Gross, E., 2004. Time-dependent density functional theory, *Annual Review of Physical Chemistry* 55: 427–455.

Marques, M. A. L., Ullrich C., Nogueira F., Rubio, A., Burke, K. and Gross, E. K. U., ed., 2006. *Time-dependent density functional theory*, volume 706 of *Lecture Notes in Physics*. Berlin: Springer.

Michalet, X., Pinaud, F., Bentolila, L. et al., 2005. Quantum dots for live cells, in vivo imaging, and diagnostics, *Science* 307: 538–544.

Mikulec, F. and Bawendi, M., 2000. Synthesis and characterization of strongly fluorescent CdTe nanocrystal colloids, in Komarneni, S and Parker, JC and Hahn, H, ed., *Nanophase and Nanocomposite Materials III*, volume 581 of *Materials Research Society Symposium Proceedings*, 139–144.

Murray, C., Norris, D. and Bawendi, M., 1993. Synthesis and characterization of nearly monodisperse CdE (E = S, Se, Te) semiconductor nanocrystallites, *Journal of the American Chemical Society* 115: 8706–8715.

Ouyang, J., Zaman, M. B., Yan, F. J. et al., 2008. Multiple families of magic-sized CdSe nanocrystals with strong bandgap photoluminescence via noninjection one-pot syntheses, *Journal of Physical Chemistry C* 112: 13805–13811.

Parr, R. G. and Yang, W., 1989. *Density-functional theory of atoms and molecules*. New York: Oxford University Press.

Peng, X., Manna, L., Yang, W. et al., 2000. Shape control of CdSe nanocrystals, *Nature* 404: 59–61.

Peng, X., Schlamp, M., Kadavanich, A. and Alivisatos, A., 1997. Epitaxial growth of highly luminescent CdSe/CdS core/shell nanocrystals with photostability and electronic accessibility, *Journal of the American Chemical Society* 119: 7019–7029.

Peng, Z. and Peng, X., 2001. Formation of high-quality CdTe, CdSe, and CdS nanocrystals using CdO as precursor, *Journal of the American Chemical Society* 123: 183–184.

Perdew, J., Burke, K. and Ernzerhof, M., 1996. Generalized gradient approximation made simple, *Physical Review Letters* 77: 3865–3868.

Perdew, J. and Zunger, A., 1981. Self-interaction correction to density functional approximations for many-electron systems, *Physical Review B* 23: 5048–5079.

Pradhan, N., Xu, H. and Peng, X., 2006. Colloidal CdSe quantum wires by oriented attachment, *Nano Letters* 6: 720–724.

Puzder, A., Williamson, A., Gygi, F. and Galli, G., 2004. Self-healing of CdSe nanocrystals: First-principles calculations, *Physical Review Letters* 92.

Rabani, E., 2001. Structure and electrostatic properties of passivated CdSe nanocrystals, *Journal of Chemical Physics* 115: 1493–1497.

Reiss, P., Bleuse, J. and Pron, A., 2002. Highly luminescent CdSe/ZnSe core/shell nanocrystals of low size dispersion, *Nano Letters* 2: 781–784.

Runge, E. and Gross, E., 1984. Density-functional theory for time-depnedent systems, *Physical Review Letters* 52: 997–1000.

Sarkar, P. and Springborg, M., 2003. Density-functional study of size-dependent properties of CdmSen clusters, *Physical Review B* 68.

Shiang, J., Kadavanich, A., Grubbs, R. and Alivisatos, A., 1995. Symmetry of annealed wurtzite CdSe nanocrystals - Assignment to the C-3v point group, *Journal of Physical Chemistry* 99: 17417–17422.

Soler, J., Artacho, E., Gale, J. et al., 2002. The SIESTA method for ab initio order-N materials simulation, *Journal of Physics-Condensed Matter* 14: 2745–2779.

Soloviev, V., Eichhofer, A., Fenske, D. and Banin, U., 2000. Molecular limit of a bulk semiconductor: Size dependence of the "band gap" in CdSe cluster molecules, *Journal of the American Chemical Society* 122: 2673–2674.

Talapin, D., Haubold, S., Rogach, A., Kornowski, A., Haase, M. and Weller, H., 2001. A novel organometallic synthesis of highly luminescent CdTe nanocrystals, *Journal of Physical Chemistry B* 105: 2260–2263.

Tessler, N., Medvedev, V., Kazes, M., Kan, S. and Banin, U., 2002. Efficient near-infrared polymer nanocrystat light-emitting diodes, *Science* 295: 1506–1508.

Troullier, N. and Martins, J., 1991. Efficient pseudopotentials for plane-wave calculations, *Physical Review B* 43: 1993–2006.

Vanderbilt, D., 1990. Soft self-consistent pseudopotentials in a generalized eigenvalue formalism, *Physical Review B* 41: 7892–7895.

Yu, W., Qu, L., Guo, W. and Peng, X., 2003a. Experimental determination of the extinction coefficient of CdTe, CdSe, and CdS nanocrystals, *Chemistry of Materials* 15: 2854–2860.

Yu, W., Wang, Y. and Peng, X., 2003b. Formation and stability of size-, shape-, and structure-controlled CdTe nanocrystals: Ligand effects on monomers and nanocrystals, *Chemistry of Materials* 15: 4300–4308.

Zhang, H., Cui, Z., Wang, Y. et al., 2003. From water-soluble CdTe nanocrystals to fluorescent nanocrystal-polymer transparent composites using polymerizable surfactants, *Advanced Materials* 15: 777.

Zhang, J., Wang, X., Xiao, M., Qu, L. and Peng, X., 2002. Lattice contraction in free-standing CdSe nanocrystals, *Applied Physics Letters* 81: 2076–2078.

Zhong, X., Zhang, Z., Liu, S., Han, M. and Knoll, W., 2004. Embryonic nuclei-induced alloying process for the reproducible synthesis of blue-emitting ZnxCd1-xSe nanocrystals with long-time thermal stability in size distribution and emission wavelength, *Journal of Physical Chemistry B* 108: 15552–15559.

Acknowledgments

I thank Miguel Marques for the critical reading of the manuscript. I acknowledge financial support from the EC Network of Excellence NANOQUANTA (NMP4-CT-2004-500198) and the French ANR (JC05_46741 and NT05-3_43900).

Figures

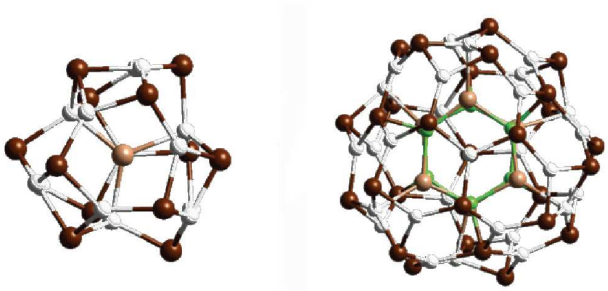

Figure 1: Structures of the $(CdSe)_n$ corecage nanoparticles calculated to be most stable by Kasuya et al. (Kasuya et al. 2004), viewed down a threefold symmetry axis. a) $(CdSe)_{13}$ has four-membered and 10 six-membered rings on the cage of 12 Se (dark brown) and 13 Cd (white) ions with a Se (light brown) ion inside. b) $(CdSe)_{34}$ has a truncated-octahedral morphology formed by a $(CdSe)_{28}$ cage (Se, dark brown; Cd, white) with 6 four-membered and 8×3 six-membered rings. A $(CdSe)_6$ cluster (Se, light brown; Cd, green) encapsulated inside this cage provides additional network and stability. Reprinted by permission from Macmillan Publishers Ltd: Nature Materials (Kasuya et al. 2004), copyright 2004.

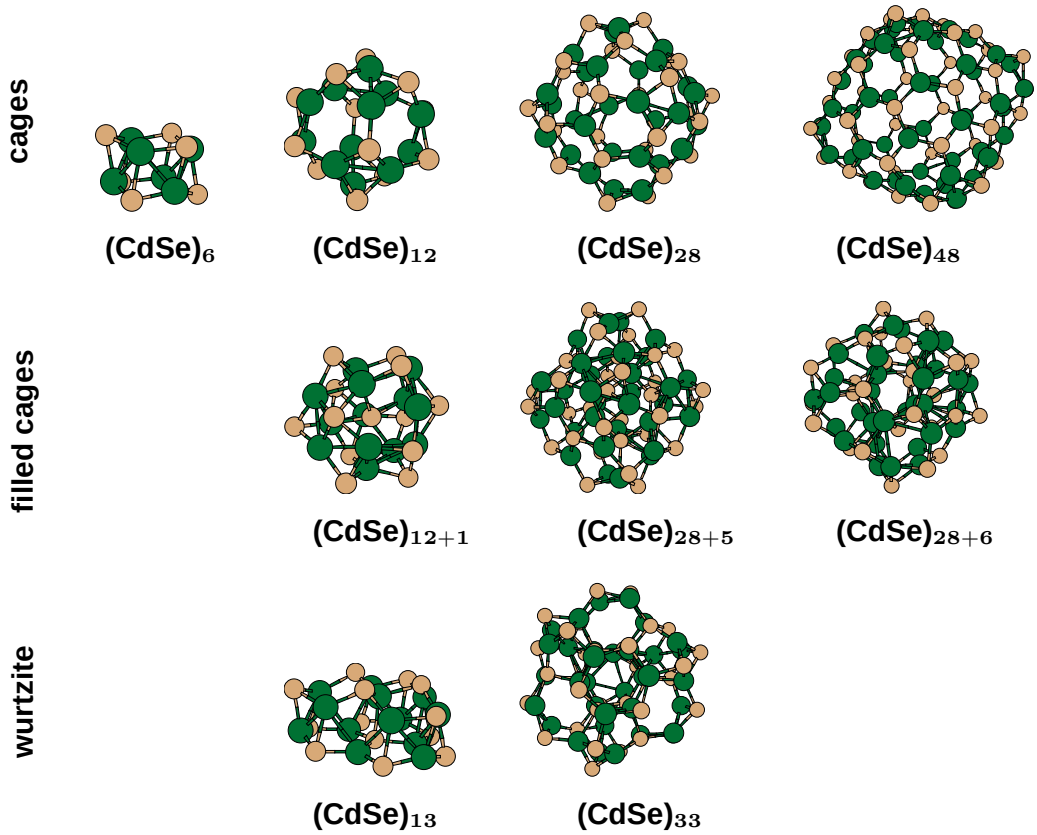

Figure 2: Examples of relaxed cages, relaxed filled cages and relaxed wurtzite structures of $(CdSe)_n$ with a diameter smaller than 2 nm. Cd atoms are in green and Se atoms are in beige. From Ref. (Botti and Marques 2007).

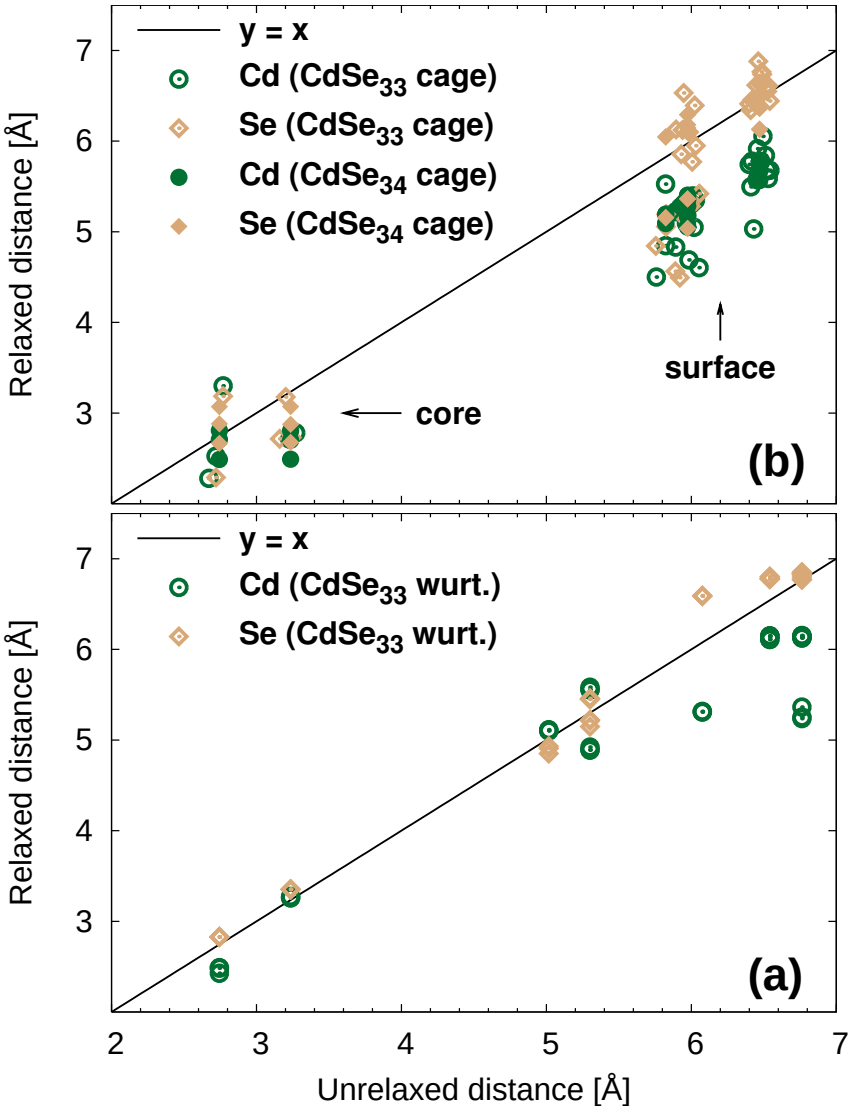

Figure 3: Distance of Cd atoms (circles) and Se atoms (diamonds) from the center of the cluster after geometry optimization, as a function of their distance before optimization. An atom that lies on the straight line $y = x$ did not change its position. In panel (a) results of the analysis for $(CdSe)_{33,34}$ core-cage clusters, in panel (b) for the $(CdSe)_{33}$ wurtzite cluster. From Ref. (Botti and Marques 2007).

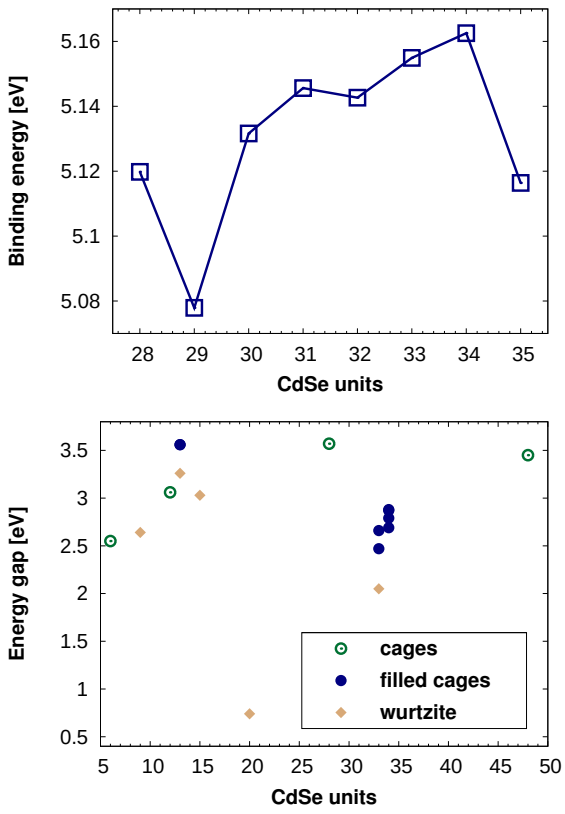

Figure 4: Left panel: Calculated binding energies per CdSe unit as a function of the number of CdSe units (data from (Kasuya et al. 2004)). The binding energies are calculated per CdSe molecule of $(CdSe)_n$ composed of a cage-like $(CdSe)_{28}$ with $(CdSe)_m$ inside ($n = 28 + m$, $m = 0, 1, \ldots, 7$). Right panel: HOMO-LUMO gaps as a function of the number of CdSe units (from Ref. (Botti and Marques 2007)). The empty (filled) circles refer to cage (core-cage) clusters, while the diamonds refer to wurtzite-based structures.

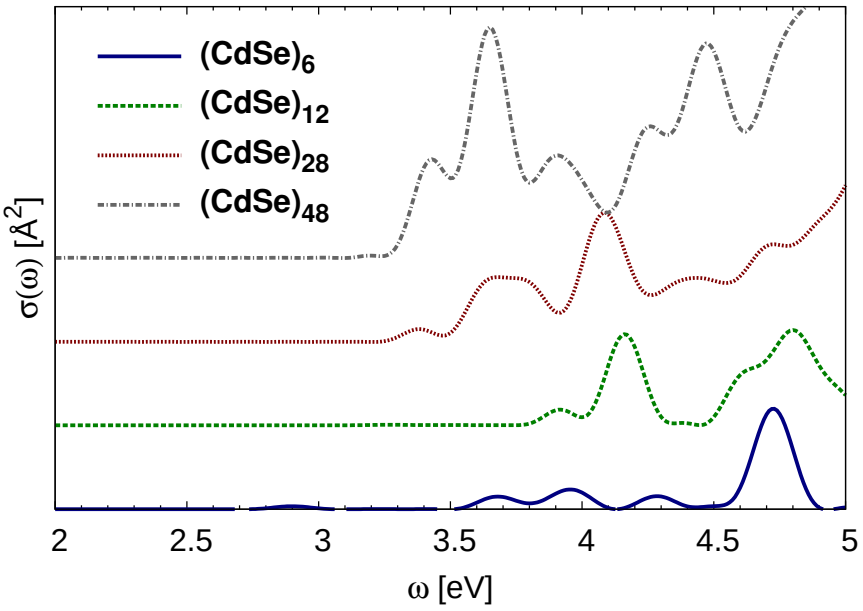

Figure 5: Calculated photoabsorption cross section $\sigma(\omega)$ of the empty cages $(CdSe)_6$, $(CdSe)_{12}$, $(CdSe)_{28}$ and $(CdSe)_{48}$ from Ref.(Botti and Marques 2007). The spectra were shifted vertically for visualization purposes.

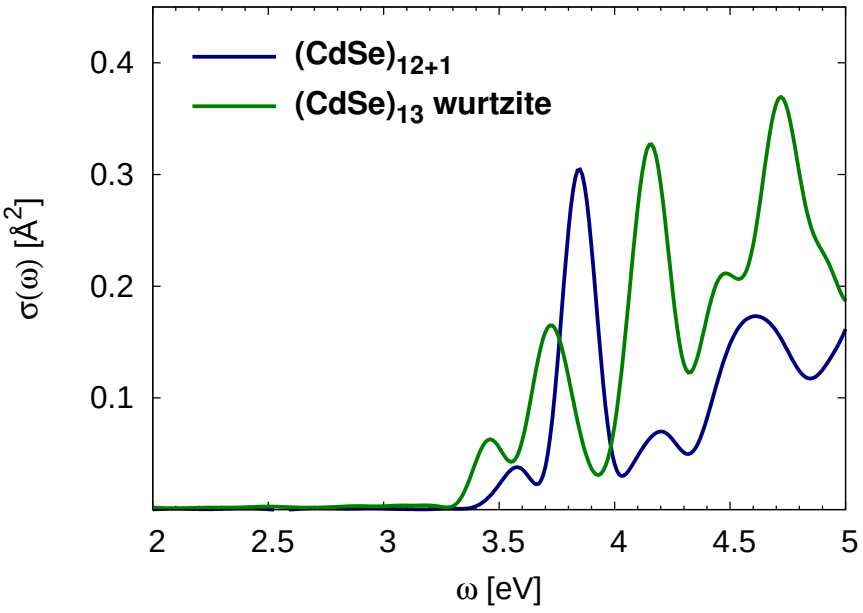

Figure 6: Calculated photoabsorption cross section $\sigma(\omega)$ of the isomers of $(CdSe)_{13}$ from Ref. (Botti and Marques 2007).

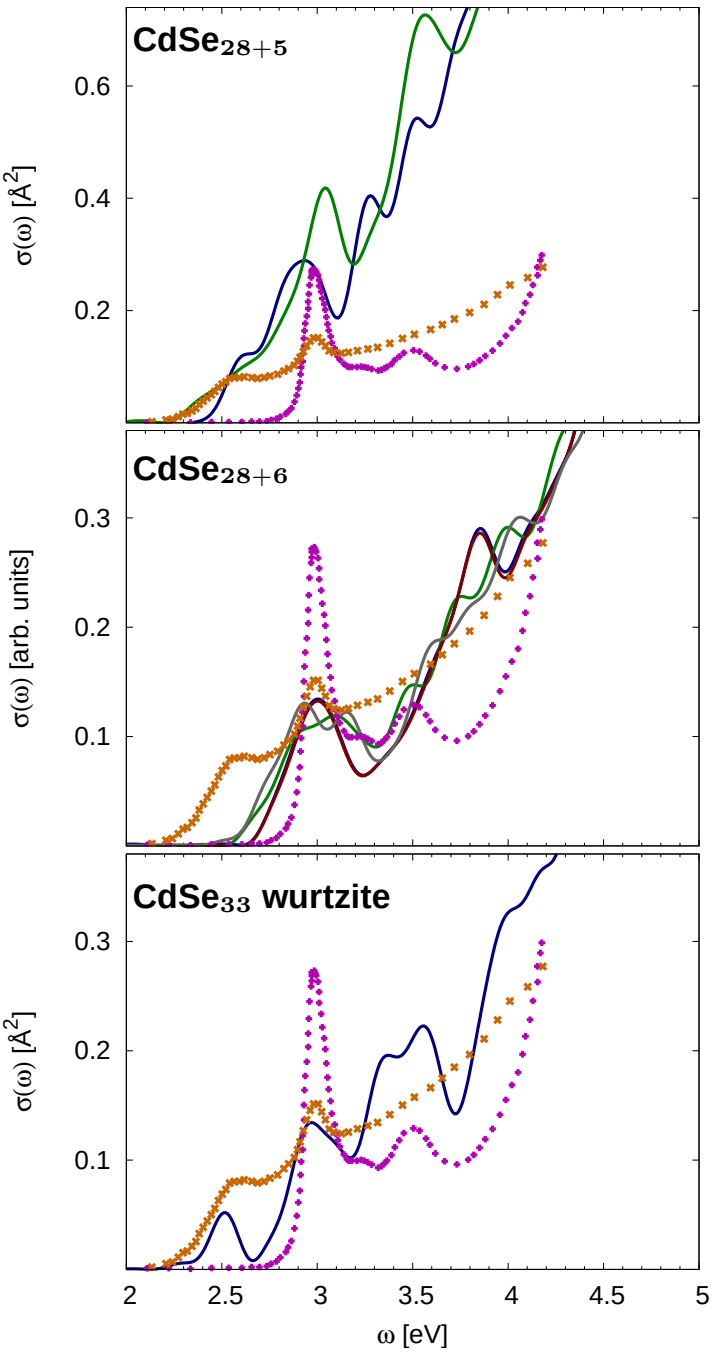

Figure 7: Photoabsorption cross section $\sigma(\omega)$ of the isomers of $(CdSe)_{33,34}$. The experimental data (Kasuya et al. 2004) in arbitrary units (magenta dots: sample I at 45°C and orange crosses: sample II at 80°C) are compared with calculated spectra from Ref. (Botti and Marques 2007). The different solid curves correspond to distinct relaxed geometries obtained starting from different filled cages.